

Higher-order two-mode and multimode entanglement in Raman processes

Sandip Kumar Giri,^{1,2} Biswajit Sen,³ Anirban Pathak,⁴ and Paresh Chandra Jana²

¹*Department of Physics, Panskura Banamali College, Panskura-721152, India*

²*Department of Physics, Vidyasagar University, Midnapore-721102, India*

³*Department of Physics, Vidyasagar Teachers' Training College, Midnapore-721101, India*

⁴*Jaypee Institute of Information Technology, A-10, Sector-62, Noida, UP-201307, India*

(Received 22 September 2015; published 25 January 2016)

The existence of higher-order entanglement in the stimulated and spontaneous Raman processes is established using the perturbative solutions of the Heisenberg equations of motion for various field modes that are obtained using the Sen-Mandal technique and a fully quantum mechanical Hamiltonian that describes the stimulated and spontaneous Raman processes. Specifically, the perturbative Sen-Mandal solutions are exploited here to show the signature of the higher-order two-mode and multimode entanglement. In some special cases, we have also observed higher-order entanglement in the partially spontaneous Raman processes. Further, it is shown that the depth of the nonclassicality indicators (parameters) can be manipulated by the specific choice of coupling constants, and it is observed that the depth of nonclassicality parameters increases with the order.

DOI: [10.1103/PhysRevA.93.012340](https://doi.org/10.1103/PhysRevA.93.012340)

I. INTRODUCTION

With the advent of quantum computation and communication, entanglement has appeared as a very important resource [1–4]. For example, its essential role in many processes, such as teleportation [1], dense coding [2], quantum information splitting [3], etc., is now well established. In short, entangled states are required to perform various important tasks related to quantum information processing. Entanglement is produced in many physical systems and there exists a large number of criteria for detection of entanglement ([5] and references therein). The first inseparability criterion was proposed by Peres [6] in 1996. Since then several inseparability inequalities have been reported for two-mode and multimode states [7–19]. For the present study, we have mostly used higher-order version of two criteria of Hillery and Zubairy [11,12]. To be precise, we have used these criteria to investigate the existence of higher-order entanglement in Raman processes, as depicted in Fig. 1.

From Fig. 1 we can easily observe that the scheme illustrated here is essentially a sequential double Raman process [15]. Nonclassical properties of this system have been studied for a long time (for a review see Ref. [20]). Initial studies on this system were restricted to the short-time approximation [21,22]. However, recently nonclassical properties of this system have been investigated by some of us [23,24] using different approaches other than short-time approximation, but the possibility of observing higher-order entanglement is not investigated in any of the existing studies. Further, several applications of Raman processes have been reported in the recent past [25–32]. Specifically, quantum repeaters having applications in long-distance quantum communication have been built using the spontaneous Raman process [25,26], laser cooling of solids [27], construction of THz source [28], quantitative chemical imaging [29], fast molecular spectral imaging of tissue [30], construction of quantum random number generator [31], and highly sensitive medical imaging [32] have been reported using stimulated Raman process. Moreover, higher-order nonclassicality in different physical systems has also been reported experimentally [33–36] and theoretically [37–40]. Further, in Ref. [33] it is shown that higher-order nonclassicality criteria can easily detect some weak nonclassicalities

that are difficult to be detected by lower-order criteria of nonclassicality (cf. Fig. 4 of Ref. [33] and the corresponding discussions). Keeping these facts in mind, the present paper aims to investigate the possibility of higher-order entanglement in the spontaneous, partially spontaneous, and stimulated Raman processes. Further, the effect of the phase of the pump mode on the observed higher-order entanglement is also analyzed.

In what follows, Raman process is described as shown in Fig. 1 and a completely quantum mechanical description of the system is used to obtain analytic expressions for the time evolution of the various field modes involved in the process. The expressions are obtained using a perturbative method known as the Sen-Mandal method [41–44]. Subsequently, the expressions obtained using this method and Hillery-Zubairy criteria [11,12] are used to investigate the existence of multimode entanglement and higher-order two-mode entanglement. Interestingly, the investigation has revealed the existence of multimode entanglement (which is essentially higher order as is witnessed via higher-order correlation function) and higher-order two-mode entanglement involving various modes present in the Raman process.

The remaining part of the present paper is organized as follows. In Sec. II, the Hamiltonian of stimulated Raman processes and its operator solution are briefly described. In Sec. III, the solution is used to show the existence of higher-order two-mode, three-mode, and four-mode entanglement and the effect of phase of the pump mode on the higher-order entanglement. Finally, the paper is concluded in Sec. IV.

II. MODEL HAMILTONIAN

A completely quantum mechanical description of stimulated and spontaneous Raman processes described in Fig. 1 is given by the Hamiltonian [21,24,41–44,46,47]

$$H = \omega_a a^\dagger a + \omega_b b^\dagger b + \omega_c c^\dagger c + \omega_d d^\dagger d + g(ab^\dagger c^\dagger + \text{H.c.}) + \chi(acd^\dagger + \text{H.c.}), \quad (1)$$

where H.c. stands for the Hermitian conjugate. Throughout the present paper, we use $\hbar = 1$. The annihilation (creation) operators $a(a^\dagger)$, $b(b^\dagger)$, $c(c^\dagger)$, $d(d^\dagger)$ correspond to the laser

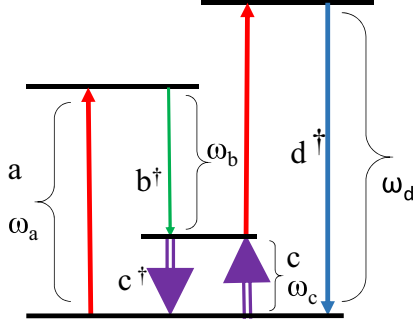


FIG. 1. Two-photon stimulated Raman scheme. The pump photon is converted into a Stokes photon and a phonon. The pump photon can also mix with a phonon to produce an anti-Stokes photon.

(pump) mode, Stokes mode, vibration (phonon) mode, and anti-Stokes mode, respectively. They obey the well-known bosonic commutation relations. The frequencies ω_a , ω_b , ω_c , and ω_d correspond to the frequencies of pump mode a , Stokes mode b , vibration (phonon) mode c , and anti-Stokes mode d , respectively. The parameters g and χ are the Stokes and anti-Stokes coupling constants, respectively. The coupling constant g (χ) denotes the strength of coupling between the Stokes (anti-Stokes) mode and the vibrational (phonon) mode and depends on the actual interaction mechanism. The dimension of g and χ are that of frequency and consequently gt and χt are dimensionless. Further, gt and χt are very small compared to unity. Further, we would like to note that in our present study, only one vibration (phonon) mode has been considered for the mathematical simplicity.

In order to study the possibility of the existence of higher-order entanglement, we need simultaneous solutions of the following Heisenberg operator equations of motion for various field operators:

$$\begin{aligned}\dot{a} &= -i(\omega_a a + gbc + \chi cd), \\ \dot{b} &= -i(\omega_b b + gac^\dagger), \\ \dot{c} &= -i(\omega_c c + gab^\dagger + \chi a^\dagger d), \\ \dot{d} &= -i(\omega_d d + \chi ac).\end{aligned}\quad (2)$$

$$\begin{aligned}a(t) &= f_1 a(0) + f_2 b(0)c(0) + f_3 c^\dagger(0)d(0) + f_4 a^\dagger(0)b(0)d(0) + f_5 a(0)b(0)b^\dagger(0) + f_6 a(0)c^\dagger(0)c(0) \\ &\quad + f_7 a(0)c^\dagger(0)c(0) + f_8 a(0)d^\dagger(0)d(0), \\ b(t) &= g_1 b(0) + g_2 a(0)c^\dagger(0) + g_3 a^2(0)d^\dagger(0) + g_4 c^{\dagger 2}(0)d(0) + g_5 b(0)c(0)c^\dagger(0) + g_6 b(0)a(0)a^\dagger(0), \\ c(t) &= h_1 c(0) + h_2 a(0)b^\dagger(0) + h_3 a^\dagger(0)d(0) + h_4 b^\dagger(0)c^\dagger(0)d(0) + h_5 c(0)a(0)a^\dagger(0) \\ &\quad + h_6 c(0)b(0)b^\dagger(0) + h_7 c(0)d^\dagger(0)d(0) + h_8 c(0)a^\dagger(0)a(0), \\ d(t) &= l_1 d(0) + l_2 a(0)c(0) + l_3 a^2(0)b^\dagger(0) + l_4 b(0)c^2(0) + l_5 c^\dagger(0)c(0)d(0) + l_6 a(0)a^\dagger(0)d(0).\end{aligned}\quad (3)$$

The parameters f_i , g_i , h_i and l_i are computed using the initial boundary conditions. In order to obtain the solutions we use the boundary conditions at $t = 0$, i.e., $f_1(0) = g_1(0) = h_1(0) = l_1(0) = 1$ and $f_i(0) = g_i(0) = h_i(0) = l_i(0) = 0$ (for $i = 2, 3, 4, 5, 6, 7$, and 8). This is so because in the absence of

The above set of equations (2) are coupled nonlinear differential equations of field operator and are not exactly solvable in the closed analytical form under weak pump condition. However, for the very strong pump, the operator a can be replaced by a c number and these equations (2) are exactly solvable in that case [22].

In order to solve these equations under weak pump approximation, we have used Sen-Mandal perturbative approach [41–44]. The specific reason behind choosing this particular perturbation technique underlies in the fact that the solutions obtained using this approach are more general than the solutions obtained for the same system using the well-known short-time (or short-length) approximation. To be precise, short-time (short-length) approximated solution can be obtained as a special case of the Sen-Mandal perturbative solution if we neglect all the terms beyond certain power of rescaled time (length). For example, neglecting the terms beyond quadratic or cubic powers in rescaled time (length) we obtain a second- or third-order short-time (short-length) solution. Further, the solutions obtained using this approach may be used to detect nonclassicality that is not detected by short-time (short-length) solutions. For example, in an asymmetric nonlinear optical coupler in codirectional propagation of radiation field the short-length solution failed to detect squeezing in fundamental and second harmonic modes. However, they were observed when investigated using the Sen-Mandal solution (cf. Table 1 of Ref. [45]). Similarly, in the same system, the Sen-Mandal solution successfully detected antibunching in fundamental and second harmonic modes, which short-time solution could not. Similarly, for contradirectional propagation in an asymmetric nonlinear optical coupler intermodal squeezing was observed with the Sen-Mandal solution, but it was not observed with short-length solution (cf. Table 1 of Ref. [40]).

Here we have not elaborately discussed the methods followed to obtain the Sen-Mandal perturbative solution as the details of the calculations are already given in our previous papers [41–44]. Here, we first note that under weak pump approximation, the solutions of Eq. (2) are assumed in the following form:

the interaction (i.e., for $g = \chi = 0$) the parameters f_i , g_i , h_i , and l_i are zero except f_1 , g_1 , h_1 , and l_1 . Under these initial conditions the corresponding solutions for $f_i(t)$, $g_i(t)$, $h_i(t)$, and $l_i(t)$ are already reported in our earlier work [24]. The same is included here as Appendix.

In order to obtain the above assumed solutions, we have used the time evolution of the operator $a(t)$ as

$$a(t) = \exp(iHt)a(0)\exp(-iHt). \quad (4)$$

Expanding Eq. (4), we obtain

$$a(t) = a(0) + it[H, a(0)] + \frac{(it)^2}{2!}[H, [H, a(0)]] + \frac{(it)^3}{3!}[H, [H, [H, a(0)]]] + \dots \quad (5)$$

The commutators present in the right-hand side of Eq. (5) provide the time evolution of the operator $a(t)$. It is to be noted that in our method we neglect the terms beyond the quadratic powers of the interaction constants g and χ , but we do not impose any restriction on time t . Specifically, our assumed solution contains all the terms arising from the infinite series (5), provided that the terms are not of higher power (higher than quadratic) in g and χ . Once an assumed solution for a specific mode is obtained in this way, the assumed solution is substituted in the Heisenberg's equation of motion for that mode obtained using the given Hamiltonian, subsequently the coefficients of the similar terms are compared. This leads to a set of coupled ordinary differential equations involving f_i, g_i, h_i , and l_i , which are subsequently solved using the standard methods to obtain the final analytic solution. The presence of the additional terms provides an advantage to the present technique over the conventional short-time method. For example, the second and third terms in the right-hand side of Eq. (5) are equivalent to the first and second derivative of operator a , respectively. Thus, a second-order short-time solution do not contain the terms arising from the third term in the right-hand side of Eq. (5) while the solution assumed here even contains the terms (up to second order in coupling constants g and χ) arising from third and higher terms [terms that are not shown in the series (5)]. For example, f_4 is proportional to $(\Delta\omega_1 + \Delta\omega_2)\chi g t^3$, where $\Delta\omega_1 = \omega_b + \omega_c - \omega_a$ and $\Delta\omega_2 = \omega_a + \omega_c - \omega_d$ are the detunings and are usually very small. In the present work, we have chosen $|\Delta\omega_1| = 0.1$ MHz and $|\Delta\omega_2| = 0.19$ MHz. Hence our solutions are valid beyond t^2 and thus beyond the region of validity of a short-time approximated solution as in that we neglect the terms beyond $(gt)^2$ and $(\chi t)^2$. In this way our solutions are more general than the solutions from short-time approximation. Recently, it is established by some of us that the improved solutions by the Sen-Mandal technique can detect several nonclassical characters that are not observed using the solutions from short-time approximations [38,40–43].

III. HIGHER-ORDER INTERMODAL ENTANGLEMENT

In order to investigate the higher-order entanglement in spontaneous and stimulated Raman processes, we assume that all photon and phonon modes are initially coherent. In other words, the composite boson field consisting of photons and phonon is in an initial state, which is product of coherent states. Therefore, the composite coherent state arises from the product of the coherent states $|\alpha_1\rangle, |\alpha_2\rangle, |\alpha_3\rangle$, and $|\alpha_4\rangle$, which are the eigenkets of a, b, c , and d , respectively. Thus, the initial

composite state is

$$|\psi(0)\rangle = |\alpha_1\rangle \otimes |\alpha_2\rangle \otimes |\alpha_3\rangle \otimes |\alpha_4\rangle. \quad (6)$$

This particular choice of the initial state is justified, because in the radiation photon modes (i.e., pump, Stokes, and anti-Stokes modes) it is natural to assume initial coherent states when (ideal) laser beams are used. However, the phonon mode can be assumed as both coherent or chaotic (as is done in our earlier work (cf. Secs. III and IV of Ref. [23]). Here, we have restricted ourselves to the situation where the initial state of the phonon mode is in the coherent state, which essentially implies coherent scattering, and provides calculational convenience.

It is clear that the initial state is separable. Now the field operator $a(0)$ operating on such a composite coherent state gives rise to the complex eigenvalue α_1 . Hence we have,

$$a(0)|\psi(0)\rangle = \alpha_1|\psi(0)\rangle, \quad (7)$$

where $|\alpha_1|^2$ is the number of input photons in the pump mode. In a similar fashion, we can also describe three more complex amplitudes $\alpha_2(t), \alpha_3(t)$, and $\alpha_4(t)$ corresponding to the Stokes, vibrational (phonon), and anti-Stokes field mode operators b, c , and d , respectively. It is clear that for a spontaneous process, the complex amplitudes except for the pump mode, are necessarily zero. Thus, in the spontaneous Raman process, $\alpha_2 = \alpha_3 = \alpha_4 = 0$ and $\alpha_1 \neq 0$. For partially spontaneous process [23], the complex amplitude α_1 and any one (two) of the remaining three eigenvalues are nonzero while the other two (one) complex amplitudes is zero. In the present investigation, we consider that the eigenvalue corresponding to the pump mode is complex i.e., $\alpha_1 = |\alpha_1|e^{-i\phi}$, where ϕ is the phase angle, but the other eigenvalues [i.e., eigenvalues for the Stokes, vibrational (phonon) and anti-Stokes modes] are real.

A. Higher-order two-mode entanglement

In order to investigate the higher-order two-mode entanglement, we use two criteria due to Hillery and Zubairy [11,12]. The first criteria of Hillery and Zubairy is

$$E_{i,j}^{n,m} = \langle i^{\dagger n} i^n j^{\dagger m} j^m \rangle - |\langle i^n j^{\dagger m} \rangle|^2 < 0, \quad (8)$$

and the second criterion is

$$E_{i,j}^{m,m} = \langle i^{\dagger n} i^n \rangle \langle j^{\dagger m} j^m \rangle - |\langle i^n j^m \rangle|^2 < 0. \quad (9)$$

where i and j are any two arbitrary operators and $i, j \in \{a, b, c, d\} \forall i \neq j$. Here m and n are the positive integers and the lowest possible values of m and n are $m = n = 1$, which corresponds to the normal (lowest) order intermodal entanglement. A quantum state is said to be higher-order entangled (bipartite) if it is found to satisfy the Eq. (8) and/or Eq. (9) for any choice of the integers m and n satisfying $m + n \geq 3$. From here onward we will refer to these criteria (8) and (9) as HZ-1 criterion and HZ-2 criterion, respectively. More specifically, a higher-order entangled state is one that is witnessed via a higher-order (order $k > 2$) correlation function and as per this definition all multipartite (multimode) entangled states are also higher-order entangled.

Before we proceed further, we note that these two criteria are only sufficient (not necessary) for detection of entanglement. Keeping this fact in mind, we have applied

both of these two criteria to investigate the existence of higher-order intermodal entanglement between various modes and have observed higher-order intermodal entanglement in various situations. In what follows, we have also investigated the possibility of observing three-mode and four-mode entanglement.

Let us first investigate the possibility of two mode entanglement in Raman process using HZ-1 and HZ-2 criteria. From Eqs. (3), (6), (8), and (9), we obtain the expression for the

intermodal entanglement in pump and Stokes mode as

$$\begin{pmatrix} E_{a,b}^{n,m} \\ E_{a,b}^{m,m} \end{pmatrix} = |f_2|^2 m(m|\alpha_1|^{2(n+1)}|\alpha_2|^{2(m-1)} \mp n|\alpha_1|^{2n}|\alpha_2|^{2m}) \\ + |f_3|^2 n^2 |\alpha_1|^{2(n-1)} |\alpha_2|^{2m} |\alpha_4|^2. \quad (10)$$

In the similar manner, for the remaining cases, we obtain expressions for $E_{i,j}^{n,m}$ and $E_{i,j}^{m,m}$: $i, j \in \{a, b, c, d\} \forall i \neq j$ using HZ-1 and HZ-2 criteria as follows

$$\begin{pmatrix} E_{b,c}^{n,m} \\ E_{b,c}^{m,m} \end{pmatrix} = |g_2|^2 |\alpha_2|^{2(n-1)} |\alpha_3|^{2(m-1)} \{n^2(1 \pm 2m)|\alpha_1|^2 |\alpha_3|^2 + m^2(1 \pm 2n)|\alpha_1|^2 |\alpha_2|^2 \\ \pm m^2 n^2 |\alpha_1|^2 \mp mn|\alpha_2|^2 |\alpha_3|^2\} + |h_3|^2 m^2 |\alpha_2|^{2n} |\alpha_3|^{2(m-1)} |\alpha_4|^2 \\ \pm |\alpha_2|^{2(n-2)} |\alpha_3|^{2(m-2)} mn \left[g_1 g_2^* |\alpha_2|^2 |\alpha_3|^2 \alpha_1^* \alpha_2 \alpha_3 + h_2 h_3^* m |\alpha_2|^2 |\alpha_3|^2 \alpha_1^* \alpha_2^* \alpha_4^* \right. \\ \left. + g_1 g_4^* |\alpha_2|^2 \alpha_2 \alpha_3^* \alpha_4^* (2|\alpha_3|^2 + m - 1) + h_1^* h_2 h_3 (m - 1) |\alpha_1|^2 |\alpha_2|^2 \alpha_3^* \alpha_4^* \right. \\ \left. + g_1^2 g_2^* \alpha_1^* \alpha_2^* \alpha_3^2 \left\{ \frac{1}{2}(m-1)(n-1) + (m-1)|\alpha_2|^2 + (n-1)|\alpha_3|^2 \right\} + \text{c.c.} \right], \quad (11)$$

$$\begin{pmatrix} E_{a,c}^{n,m} \\ E_{a,c}^{m,m} \end{pmatrix} = |f_2|^2 |\alpha_1|^{2n} |\alpha_3|^{2(m-1)} m(m|\alpha_1|^2 \mp n|\alpha_3|^2) \\ + |f_3|^2 |\alpha_1|^{2(n-1)} |\alpha_3|^{2(m-1)} \{m^2(1 \pm 2n)|\alpha_1|^2 |\alpha_4|^2 + n^2(1 \pm 2m)|\alpha_3|^2 |\alpha_4|^2 \\ \mp mn|\alpha_1|^2 |\alpha_3|^2 + m^2 n^2 |\alpha_4|^2\} \pm |\alpha_1|^{2(n-2)} |\alpha_3|^{2(m-2)} mn \left[f_1 f_3^* |\alpha_1|^2 |\alpha_3|^2 \alpha_1 \alpha_3 \alpha_4^* \right. \\ \left. + h_2^* h_3 |\alpha_3|^2 \alpha_1^* \alpha_2 \alpha_4 \{m|\alpha_1|^2 - (n-1)|\alpha_3|^2\} + f_2 f_3^* |\alpha_1|^2 \alpha_2 \alpha_3^* \alpha_4^* \{n|\alpha_3|^2 - (m-1)|\alpha_1|^2\} \right. \\ \left. + f_1^* f_3^2 \alpha_1^* \alpha_3^* \alpha_4^2 \left\{ (n-1)|\alpha_3|^2 + (m-1)|\alpha_1|^2 + \frac{(m-1)(n-1)}{2} \right\} + \text{c.c.} \right], \quad (12)$$

$$\begin{pmatrix} E_{a,d}^{n,m} \\ E_{a,d}^{m,m} \end{pmatrix} = |f_3|^2 n |\alpha_1|^{2(n-1)} |\alpha_4|^{2m} (n|\alpha_4|^2 \mp m|\alpha_1|^2), \quad (13)$$

$$\begin{pmatrix} E_{c,d}^{n,m} \\ E_{c,d}^{m,m} \end{pmatrix} = |h_2|^2 n^2 |\alpha_1|^2 |\alpha_3|^{2(n-1)} |\alpha_4|^{2m} + |l_2|^2 |\alpha_3|^{2(n-1)} |\alpha_4|^{2m} [n^2 |\alpha_4|^2 \mp mn|\alpha_3|^2], \quad (14)$$

$$\begin{pmatrix} E_{bd}^{n,m} \\ E_{b,d}^{m,m} \end{pmatrix} = |g_2|^2 n^2 |\alpha_1|^2 |\alpha_2|^{2(n-1)} |\alpha_4|^{2m} \pm [l_1^* l_3 mn \alpha_1^* \alpha_2^* |\alpha_2|^{2(n-1)} \alpha_4^* |\alpha_4|^{2(m-1)} + \text{c.c.}]. \quad (15)$$

Here we would like to note that once we obtain analytic expressions for $E_{i,j}^{n,m}$ and $E_{i,j}^{m,m}$ in stimulated Raman process, it is straightforward to study the special cases: (i) spontaneous Raman process, where $\alpha_2 = \alpha_3 = \alpha_4 = 0$, but $\alpha_1 \neq 0$, and (ii) partially spontaneous Raman process, where $\alpha_1 \neq 0$ and any one (two) of the other three α_i ($i = 2, 3, 4$) is (are) nonzero. It is also easy to observe that for $m = 1, n = 1$, Eqs. (10)–(15) reduce to Eqs. (16)–(26) of Ref. [24], which were obtained earlier using lower order HZ criteria. This is indicative of the accuracy of the more general expressions reported here as Eqs. (10)–(15).

Further, it is clear from the Eqs. (10)–(15) that for spontaneous Raman process Eqs. (10)–(15) reduces to zero. Hence, for the spontaneous Raman process, no signature of intermodal entanglement is observed. To investigate the possibility of higher-order intermodal entanglement in the stimulated Raman process we have used $\chi = g = 10^4$ Hz, $|\alpha_1| = 10$, $|\alpha_2| = 8$, $|\alpha_3| = 0.01$, $|\alpha_4| = 1$ [48]. We have plot-

ted the right-hand side of (10)–(15) in Fig. 2 and Fig. 3 for $m = 1$ and $n = 1, 2$, and 3. We observed that HZ-1 criteria can detect the higher-order intermodal entanglement in the stimulated Raman process for different values of the phase angle or all phase angles of the input pump field (i.e., for $\phi = 0, \frac{\pi}{2}$, and π) for all the possible modes except pump-phonon (ac) and phonon-anti-Stokes (cd) modes. It is interesting to note that higher-order intermodal entanglement is observed in pump-Stokes mode, although in the lowest order it was not observed. Further, the figures show that the depths of the nonclassicality parameters $E_{i,j}^{n,m}$ and $E_{i,j}^{m,m}$ increase with the order. Use of HZ-1 criteria also led to similar features in the partially spontaneous Raman process (not in figure). In other words, we observed signatures of intermodal entanglement in all the cases except pump-phonon (ac) and phonon-anti-Stokes (cd) modes. As HZ-1 is only a sufficient (not necessary) criterion, it may have failed to witness entanglement, keeping this fact in mind, we have

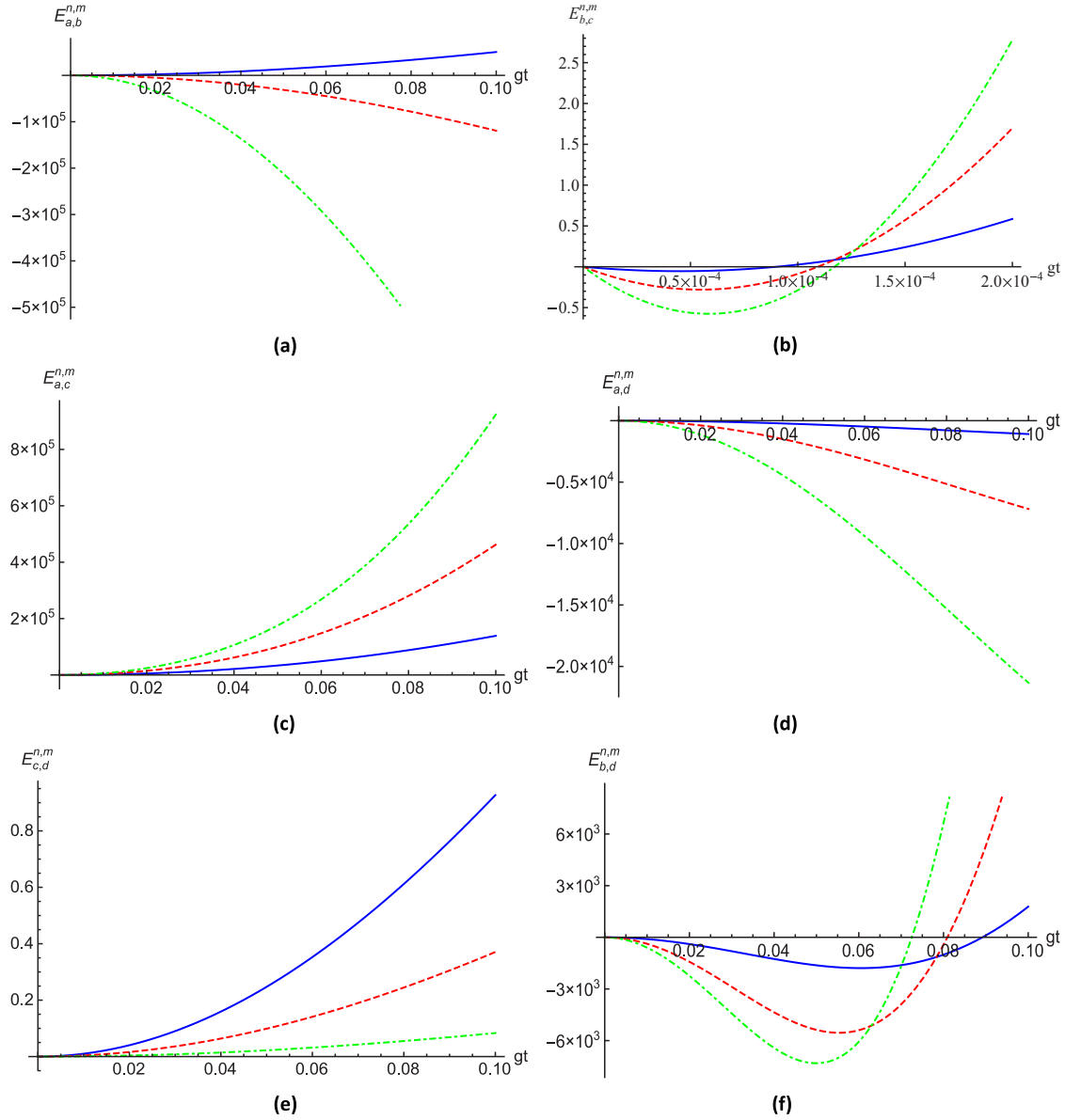


FIG. 2. Higher-order intermodal entanglement in stimulated Raman process with $|\alpha_1| = 10$, $|\alpha_2| = 8$, $|\alpha_3| = 0.01$ and $|\alpha_4| = 1$ using HZ-1 criterion is shown for different values of phase angle ($\phi = 0, \frac{\pi}{2}$, and π) in pump mode. Higher-order intermodal entanglement is observed in (a) pump-Stokes mode for phase angle 0, (b) Stokes-vibration phonon mode for phase angle $\phi = \frac{\pi}{2}$, (d) pump-anti-Stokes mode for phase angle 0, (f) Stokes-anti-Stokes mode for phase angle 0; and not observed in (c) pump-vibration phonon mode and (e) vibration phonon-anti-Stokes mode. In all the plots, the smooth line, dotted line, and dash-dotted line are used for the $m = 1$ and $n = 1, 2$, and 3 , respectively. In (e), $n = 2$ and 3 are multiplied by 10^3 and 10^6 , respectively. While in all the remaining cases, $n = 1$ and 2 are shown 1500 and 50 times, respectively. All the quantities plotted here and in the following plots are dimensionless.

plotted the right-hand side of Eq. (10)–(15) using HZ-2 criteria (see Fig. 3). It is interesting to note that HZ-2 criterion can detect the higher-order intermodal entanglement in pump-phonon (ac) mode for phase angle $\phi = \frac{\pi}{2}$, which was not detected by HZ-1 criterion, in the stimulated and partial spontaneous Raman processes. However, we do not observe any signature of higher-order intermodal entanglement for spontaneous Raman process. Thus, the stimulated Raman process provides a very nice example of a physical system, which can produce higher-order entanglement.

B. Three-mode entanglement

There exists another alternative way to study the higher-order entanglement. To be precise, all multimode entanglements are essentially higher-order entanglement. In other words, three-mode entanglement always indicates higher-order entanglement. In order to investigate the three-mode entanglement, we use the following criterion [49]

$$E'_{a,b,c} = \langle N_a \rangle \langle N_b \rangle \langle N_c \rangle - |\langle abc \rangle|^2 < 0, \quad (16)$$

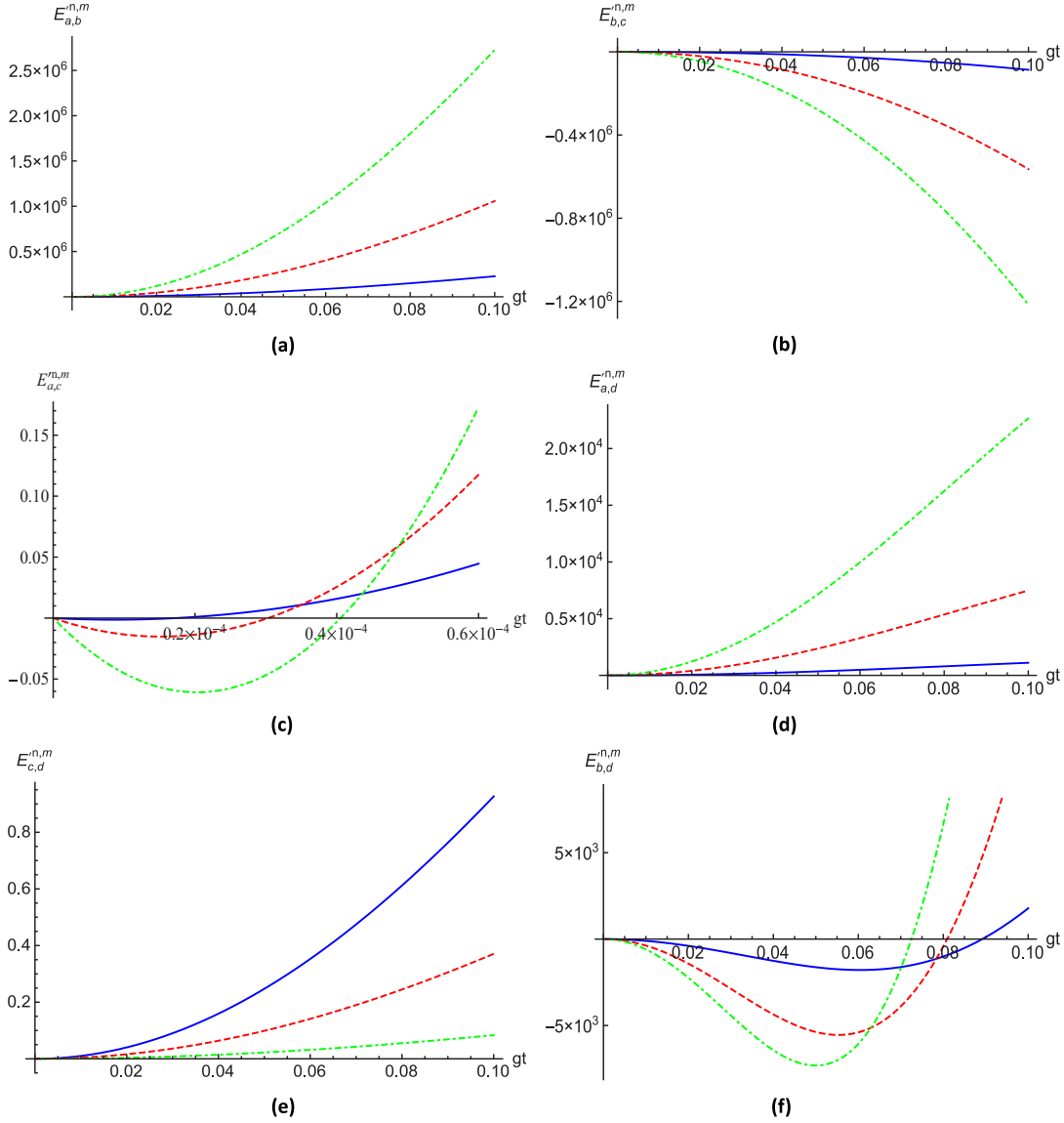


FIG. 3. Higher-order intermodal entanglement in stimulated Raman process is illustrated using HZ-2 criterion with different phase angle ($\phi = 0, \frac{\pi}{2}$, and π) in pump mode for $|\alpha_1| = 10, |\alpha_2| = 8, |\alpha_3| = 0.01$, and $|\alpha_4| = 1$. Specifically, higher-order intermodal entanglement is observed in (b) for Stokes-vibration phonon mode with phase angle $\phi = \frac{\pi}{2}$, (c) for pump-vibration phonon mode with phase angle $\phi = \frac{\pi}{2}$, and (f) for Stokes-anti-Stokes mode with phase angle $\frac{\pi}{2}$. However, in (a), (d), and (e) higher-order intermodal entanglement is not observed for pump-Stokes, pump-anti-Stokes and vibration phonon-anti-Stokes modes, respectively. The smooth, dotted and dash-dotted lines are used for $m = 1$ and $n = 1, 2$, and 3 , respectively. Here, for (e) $n = 2$ and 3 are multiplied by 10^3 and 10^6 , respectively. For all the remaining cases, $n = 1$ and 2 are shown 1500 and 50 times, respectively.

where $\langle N_a \rangle$, $\langle N_b \rangle$, and $\langle N_c \rangle$ are average value of the number operators of the pump mode Stokes mode and vibration phonon mode respectively. Using Eqs. (3), (6), and (16) we obtain

$$\begin{aligned}
 E'_{a,b,c} &= \langle N_a \rangle \langle N_b \rangle \langle N_c \rangle - |\langle abc \rangle|^2 \\
 &= |f_2|^2 |\alpha_1|^2 (5|\alpha_2|^2 |\alpha_3|^2 - |\alpha_1|^2 |\alpha_3|^2 - |\alpha_1|^2 - |\alpha_1|^2 |\alpha_2|^2) + |f_3|^2 |\alpha_2|^2 (|\alpha_1|^2 |\alpha_3|^2 - 4|\alpha_4|^2 - 3|\alpha_3|^2 |\alpha_4|^2 - 3|\alpha_1|^2 |\alpha_4|^2) \\
 &\quad - [h_1 h_2^* |\alpha_1|^2 \alpha_1^* \alpha_2 \alpha_3 + 2f_1 f_3^* |\alpha_2|^2 \alpha_1 \alpha_3 \alpha_4^* + h_2 h_3^* \alpha_1^* \alpha_2^* \alpha_4^* (2 + |\alpha_1|^2 + 2|\alpha_2|^2) + \text{c.c.}].
 \end{aligned} \tag{17}$$

For the spontaneous Raman process, Eq. (17) reduces to

$$E'_{a,b,c} = -|f_2|^2 |\alpha_1|^4, \tag{18}$$

which is clearly negative and thus indicate the existence of tripartite entanglement in the spontaneous Raman process.

To investigate the existence of three mode entanglement in the stimulated Raman process, we plot the right-hand side of the equation (17) in Fig. 4 for three different values of the phase angle of the input pump field, i.e., for $\phi = 0$ (blue smooth line), $\phi = \frac{\pi}{2}$ (red dotted line), and $\phi = \pi$ (green dash

dotted line). The negative regions of the plots clearly illustrate the existence of trimodal (higher-order) entanglement. From Fig. 4 we can clearly observe the signature of higher-order entanglement for different values of phase angle of the input pump field for stimulated and spontaneous Raman processes.

C. Four-mode entanglement

In order to investigate the four-mode entanglement we use the following criterion, which is similar to that of Li *et al.*'s

$$\begin{aligned}
 E'_{a,b,c,d} = & |f_2|^2 |\alpha_1|^2 |\alpha_4|^2 (5|\alpha_2|^2 |\alpha_3|^2 - |\alpha_1|^2 |\alpha_3|^2 - |\alpha_1|^2) \\
 & + |f_3|^2 |\alpha_2|^2 |\alpha_4|^2 (7|\alpha_1|^2 |\alpha_3|^2 - 4|\alpha_4|^2 - 3|\alpha_1|^2 |\alpha_4|^2 - 3|\alpha_3|^2 |\alpha_4|^2) \\
 & - [h_1^* h_2 |\alpha_1|^2 |\alpha_4|^2 \alpha_1 \alpha_2^* \alpha_3^* + 2f_1^* f_3 |\alpha_2|^2 |\alpha_4|^2 \alpha_1^* \alpha_3^* \alpha_4 + f_2^* f_3 \alpha_2^* \alpha_3^* \alpha_4 (|\alpha_1|^4 + 2|\alpha_2|^2 |\alpha_4|^2 - 3|\alpha_1|^2 |\alpha_4|^2) \\
 & + l_1^* l_3 |\alpha_1|^2 |\alpha_3|^2 \alpha_1^2 \alpha_2^* \alpha_4^* + h_2 h_3^* \alpha_1^2 \alpha_2^* \alpha_4^* (2|\alpha_4|^2 + |\alpha_1|^2 |\alpha_4|^2 + 2|\alpha_2|^2 |\alpha_4|^2 + 3|\alpha_3|^2 |\alpha_4|^2 - |\alpha_1|^2 |\alpha_3|^2) \\
 & + f_1 f_2^* h_1^* h_2 |\alpha_4|^2 \alpha_1^2 \alpha_2^* \alpha_3^* + 2f_1^* f_3 l_1^* l_2 |\alpha_2|^2 \alpha_1^2 \alpha_3^* \alpha_4^* + h_1^* h_4 |\alpha_1|^2 |\alpha_4|^2 \alpha_2^* \alpha_3^* \alpha_4 + \text{c.c.}]. \quad (20)
 \end{aligned}$$

In order to investigate the possibility of observing four-mode entanglement in the Raman processes, in Fig. 5 we have plotted the variation of right-hand side of Eq. (20) with the

three mode criterion [49]:

$$E'_{a,b,c,d} = \langle N_a \rangle \langle N_b \rangle \langle N_c \rangle \langle N_d \rangle - |\langle abcd \rangle|^2 < 0, \quad (19)$$

where a, b, c , and d are arbitrary operators and the negative value of $E'_{a,b,c,d}$ gives the signature of the higher-order entanglement. Now, we investigate the higher-order entanglement i.e., the entanglement among the four modes of the stimulated Raman and spontaneous Raman processes and we obtain

rescaled time gt . Quite interestingly, for appropriate choice of the phase of the pump mode, four-mode entanglement is

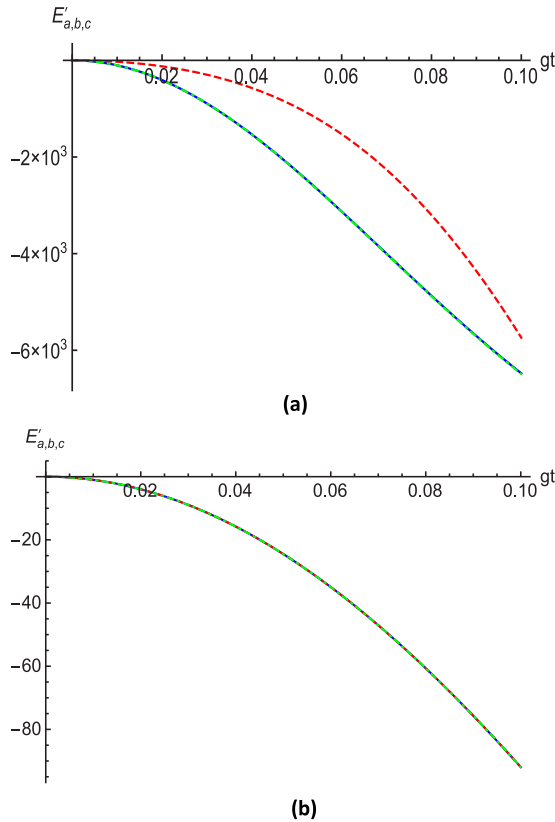


FIG. 4. The variation of three-mode entanglement among pump, Stokes and vibration phonon modes (a) for stimulated Raman process using $|\alpha_1| = 10, |\alpha_2| = 8, |\alpha_3| = 0.01, |\alpha_4| = 1$ (b) for spontaneous Raman process using $|\alpha_1| = 10, |\alpha_2| = |\alpha_3| = |\alpha_4| = 0$ with the smooth, dashed, and dash-dotted lines corresponding to $\phi = 0, \frac{\pi}{2}$, and π , respectively.

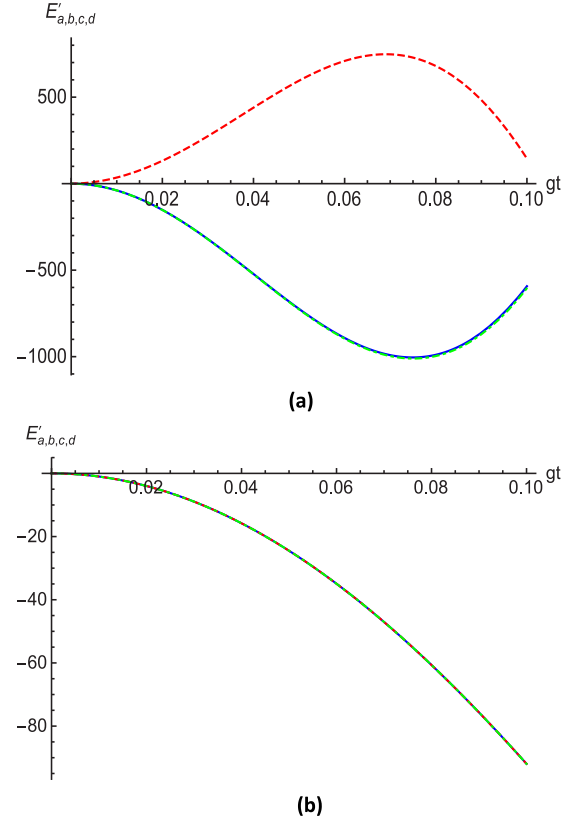


FIG. 5. Four-mode entanglement among pump, Stokes, vibration phonon, and anti-Stokes modes is depicted in (a) stimulated Raman process using $|\alpha_1| = 10, |\alpha_2| = 8, |\alpha_3| = 0.01, |\alpha_4| = 1$ (b) partial spontaneous Raman process using $|\alpha_1| = 10, |\alpha_2| = |\alpha_3| = 0$. Here, the smooth line, dashed line and dash-dotted line corresponds to $\phi = 0, \frac{\pi}{2}$, and π , respectively.

observed in both the stimulated Raman process and partially spontaneous Raman process.

IV. CONCLUSIONS

Recently, nonclassical properties of the stimulated Raman process have been extensively studied by some of the present authors [23,24]. In those studies intermodal entanglement in different modes of the stimulated Raman process was reported. Intermodal entanglement between Stokes mode and the vibration mode in the Raman processes was also reported by Kuznetsov [50]. However, higher-order entanglement was not investigated. In the present paper higher-order entanglement in stimulated the Raman process is studied in detail and the observed higher-order entanglement are illustrated through the negative regions of the Figs. 2–5. In Figs. 2 and 3, the existence of higher-order two-mode entanglement between various possible combinations of modes are illustrated using HZ-1 criterion and HZ-2 criterion, respectively. Specifically, using HZ-1 criterion, we have observed the intermodal higher-order entanglement for all the possible combinations of modes, except pump-phonon (*ac*) and phonon-anti-Stokes (*cd*) modes in the stimulated Raman process (cf. Fig. 2) and in partially spontaneous Raman processes (not shown in figure). However, we found that HZ-2 criteria can detect the signature of higher-order intermodal entanglement only in Stokes-phonon (*bc*), pump-phonon (*ac*), and Stokes-anti-Stokes (*bd*) modes in the stimulated and partially spontaneous Raman process Fig. 3, but it is interesting to note that HZ-2 criteria can detect the higher-order intermodal entanglement in pump-phonon (*ac*) mode whereas HZ-1 criteria fails to detect this. Thus, by combining the results, we have observed the existence of two-mode higher-order entanglement in stimulated and partially spontaneous Raman processes in all possible cases except in phonon-anti-Stokes (*cd*) modes. However, no signature of intermodal entanglement is observed for the spontaneous Raman process. Another interesting point is that the present investigation reveals the signature of higher-order intermodal entanglement in pump-Stokes mode (*ab*) in stimulated Raman process, but intermodal entanglement in *ab* modes was not observed in lowest order (cf. Figs. 2(a), 3(a), and 4(a) of Ref. [24]). As all the multipartite (multimode) entanglement are essentially higher-order entanglement, we investigated the possibility of observing three-mode and four-mode entanglements in Raman processes and found that trimodal entanglement can be observed among pump, Stokes, and vibration phonon mode (*abc*) in both stimulated and spontaneous Raman processes (cf. Fig. 4), and it is also possible to observe entanglement among four modes (pump, Stokes, vibration phonon, and anti-Stokes) in stimulated and partially spontaneous Raman processes (see Fig. 5). As, recently, many applications of multipartite entanglement has been proposed, we hope that the present observation on the possibility of observing multimode entanglement in the Raman process would be of help in realizing some of the recently proposed schemes that are based on multipartite entanglement. Further, it is easy to experimentally realize the Raman process and thus the results reported here can be experimentally verified using the available technologies.

Bosonic Hamiltonians similar to the one studied here frequently appear in quantum optical, optomechanical, and atomic systems. Thus, the methodology adopted here may also

be used in those systems to study the existence of nonclassical states in normal and higher-order entanglement in particular. Keeping this in mind, we conclude the present work with an expectation that this work would lead to a bunch of similar studies in other bosonic systems.

ACKNOWLEDGMENTS

S.K.G. acknowledges the financial support by the UGC, India, Government of India in the framework of the UGC minor Project No. PSW-148/14-15 (ERO). Authors thank Kishore Thapliyal for his constructive feedback on the work and his help in preparing the final figures.

APPENDIX: PARAMETERS FOR THE SOLUTIONS IN EQ. (3)

$$\begin{aligned}
f_1 &= \exp(-i\omega_a t), \\
f_2 &= \frac{g e^{-i\omega_a t}}{\Delta\omega_1} [e^{-i\Delta\omega_1 t} - 1], \\
f_3 &= -\frac{\chi e^{-i\omega_a t}}{\Delta\omega_2} [e^{i\Delta\omega_2 t} - 1], \\
f_4 &= -\frac{\chi g e^{-i\omega_a t}}{\Delta\omega_1} \left[\frac{e^{-i(\Delta\omega_1 - \Delta\omega_2)t} - 1}{\Delta\omega_1 - \Delta\omega_2} + \frac{e^{i\Delta\omega_2 t}}{\Delta\omega_2} \right] \\
&\quad - \frac{\chi g e^{-i\omega_a t}}{\Delta\omega_2} \left[\frac{e^{-i(\Delta\omega_1 - \Delta\omega_2)t} - 1}{\Delta\omega_1 - \Delta\omega_2} - \frac{e^{-i\Delta\omega_1 t}}{\Delta\omega_1} \right], \quad (A1) \\
f_5 &= \frac{g^2 e^{-i\omega_a t}}{\Delta\omega_1^2} [e^{-i\Delta\omega_1 t} - 1] + \frac{i g^2 t e^{-i\omega_a t}}{\Delta\omega_1}, \\
f_6 &= f_5, \\
f_7 &= \frac{\chi^2 e^{-i\omega_a t}}{\Delta\omega_2^2} [e^{i\Delta\omega_2 t} - 1] - \frac{i \chi^2 t e^{-i\omega_a t}}{\Delta\omega_2}, \\
f_8 &= -f_7. \\
g_1 &= \exp(-i\omega_b t), \\
g_2 &= -\frac{g e^{-i\omega_b t}}{\Delta\omega_1} [e^{i\Delta\omega_1 t} - 1], \\
g_3 &= \frac{\chi g e^{-i\omega_b t}}{\Delta\omega_2(\Delta\omega_1 - \Delta\omega_2)} [e^{i(\Delta\omega_1 - \Delta\omega_2)t} - 1] \\
&\quad - \frac{\chi g e^{-i\omega_b t}}{\Delta\omega_2 \Delta\omega_1} [e^{i\Delta\omega_1 t} - 1], \quad (A2) \\
g_4 &= \frac{\chi g e^{-i\omega_b t}}{\Delta\omega_2(\Delta\omega_1 + \Delta\omega_2)} [e^{i(\Delta\omega_1 + \Delta\omega_2)t} - 1] \\
&\quad - \frac{\chi g e^{-i\omega_b t}}{\Delta\omega_2 \Delta\omega_1} [e^{i\Delta\omega_1 t} - 1], \\
g_5 &= \frac{g^2 e^{-i\omega_b t}}{\Delta\omega_1^2} [e^{i\Delta\omega_1 t} - 1] - \frac{i g^2 t e^{-i\omega_b t}}{\Delta\omega_1}, \\
g_6 &= -g_5.
\end{aligned}$$

$$\begin{aligned}
h_1 &= \exp(-i\omega_c t) & l_1 &= \exp(-i\omega_d t) \\
h_2 &= -\frac{g e^{-i\omega_c t}}{\Delta\omega_1} [e^{i\Delta\omega_1 t} - 1] & l_2 &= \frac{\chi e^{-i\omega_d t}}{\Delta\omega_2} [e^{-i\Delta\omega_2 t} - 1] \\
h_3 &= -\frac{\chi e^{-i\omega_c t}}{\Delta\omega_2} [e^{i\Delta\omega_2 t} - 1] & l_3 &= \frac{\chi g e^{-i\omega_d t}}{\Delta\omega_1(\Delta\omega_1 - \Delta\omega_2)} [e^{i(\Delta\omega_1 - \Delta\omega_2)t} - 1] \\
h_4 &= \frac{\chi g e^{-i\omega_c t}}{\Delta\omega_2} \left[\frac{e^{i(\Delta\omega_1 + \Delta\omega_2)t} - 1}{\Delta\omega_1 + \Delta\omega_2} - \frac{e^{i\Delta\omega_1 t}}{\Delta\omega_1} \right] & & + \frac{\chi g e^{-i\omega_d t}}{\Delta\omega_2 \Delta\omega_1} [e^{-i\Delta\omega_2 t} - 1] \\
& - \frac{\chi g e^{-i\omega_c t}}{\Delta\omega_1} \left[\frac{e^{i(\Delta\omega_1 + \Delta\omega_2)t} - 1}{\Delta\omega_1 + \Delta\omega_2} - \frac{e^{i\Delta\omega_2 t}}{\Delta\omega_2} \right] & (A3) & \\
h_5 &= -\frac{g^2 e^{-i\omega_c t}}{\Delta\omega_1^2} [e^{i\Delta\omega_1 t} - 1] + \frac{i g^2 t e^{-i\omega_c t}}{\Delta\omega_1} & l_4 &= \frac{\chi g e^{-i\omega_d t}}{\Delta\omega_1(\Delta\omega_1 + \Delta\omega_2)} [e^{-i(\Delta\omega_1 + \Delta\omega_2)t} - 1] \\
h_6 &= -h_5 & & - \frac{\chi g e^{-i\omega_d t}}{\Delta\omega_2 \Delta\omega_1} [e^{-i\Delta\omega_2 t} - 1] \\
h_7 &= -\frac{\chi^2 e^{-i\omega_c t}}{\Delta\omega_2^2} [e^{i\Delta\omega_2 t} - 1] + \frac{i \chi^2 t e^{-i\omega_c t}}{\Delta\omega_2} & l_5 &= \frac{i \chi^2 t e^{-i\omega_d t}}{\Delta\omega_2} + \frac{\chi^2 e^{-i\omega_d t}}{\Delta\omega_2^2} [e^{-i\Delta\omega_2 t} - 1] \\
h_8 &= \frac{\chi^2 e^{-i\omega_c t}}{\Delta\omega_2^2} [e^{i\Delta\omega_2 t} - 1] - \frac{i \chi^2 t e^{-i\omega_c t}}{\Delta\omega_2}. & l_6 &= l_5.
\end{aligned}$$

-
- [1] C. H. Bennett, G. Brassard, C. Crepeau, R. Jozsa, A. Peres, and W. K. Wootters, *Phys. Rev. Lett.* **70**, 1895 (1993).
- [2] C. H. Bennett and S. J. Wiesner, *Phys. Rev. Lett.* **69**, 2881 (1992).
- [3] C. Shukla and A. Pathak, *Phys. Lett. A* **377**, 1337 (2013).
- [4] A. Pathak, *Elements of Quantum Computation and Quantum Communication* (CRC Press, Boca Raton, 2013).
- [5] O. Gühne and G. Tóth, *Phys. Rep.* **474**, 1 (2009).
- [6] A. Peres, *Phys. Rev. Lett.* **77**, 1413 (1996).
- [7] L.-M. Duan, G. Giedke, J. I. Cirac, and P. Zoller, *Phys. Rev. Lett.* **84**, 2722 (2000).
- [8] H. Huang and G. S. Agarwal, *Phys. Rev. A* **49**, 52 (1994).
- [9] J. Lee, M. S. Kim, and H. Jeong, *Phys. Rev. A* **62**, 032305 (2000).
- [10] R. Simon, *Phys. Rev. Lett.* **84**, 2726 (2000).
- [11] M. Hillery and M. S. Zubairy, *Phys. Rev. Lett.* **96**, 050503 (2006).
- [12] M. Hillery and M. S. Zubairy, *Phys. Rev. A* **74**, 032333 (2006).
- [13] M. Hillery, H. T. Dung, and H. Zheng, *Phys. Rev. A* **81**, 062322 (2010).
- [14] G. S. Agarwal and A. Biswas, *New J. Phys.* **7**, 211 (2005).
- [15] C. H. Raymond Ooi, Q. Sun, M. S. Zubairy, and M. O. Scully, *Phys. Rev. A* **75**, 013820 (2007).
- [16] C. H. Raymond Ooi, *Phys. Rev. A* **76**, 013809 (2007); Eyob A. Sete and C. H. Raymond Ooi, *ibid.* **85**, 063819 (2012).
- [17] A. Miranowicz, M. Bartkowiak, X. Wang, Y.-x. Liu, and F. Nori, *Phys. Rev. A* **82**, 013824 (2010).
- [18] T.-C. Wei and P. M. Goldbart, *Phys. Rev. A* **68**, 042307 (2003).
- [19] A. Miranowicz, M. Piani, P. Horodecki, and R. Horodecki, *Phys. Rev. A* **80**, 052303 (2009).
- [20] A. Miranowicz and S. Kielich, in *Advances in Chemical Physics Vol. 85*, Modern Nonlinear Optics Part 3, edited by M. Evans and S. Kielich (Wiley, New York, 1994), Chap. 10, pp. 531–626.
- [21] P. Szlachetka, S. Kielich, J. Peřina, and V. Peřinová, *J. Phys. A: Math. Gen.* **12**, 1921 (1979).
- [22] J. Peřina, *Quantum Statistics of Linear and Nonlinear Optical Phenomena* (Kluwer, Dordrecht, 1991).
- [23] A. Pathak, J. Křepelka, and J. Peřina, *Phys. Lett. A* **377**, 2692 (2013).
- [24] B. Sen, S. K. Giri, S. Mandal, C. H. R. Ooi, and A. Pathak, *Phys. Rev. A* **87**, 022325 (2013).
- [25] P. Grangier, *Nature (London)* **438**, 749 (2005).
- [26] L. M. Duan, M. Lukin, J. I. Cirac, and P. Zoller, *Nature (London)* **414**, 413 (2001).
- [27] S. C. Rand, *J. Lumin.* **133**, 10 (2013).
- [28] H. Ghosh and R. Chari, *Phys. Lett. A* **374**, 2379 (2010).
- [29] D. Fu, F.-K. Lu, X. Zhang, C. Freudiger, D. R. Pernik, G. Holtom, and X. S. Xie, *J. Am. Chem. Soc.* **134**, 3623 (2012).
- [30] Y. Ozeki, W. Umemura, Y. Otsuka, S. Satoh, H. Hashimoto, K. Sumimura, N. Nishizawa, K. Fukui, and K. Itoh, *Nature Photon.* **6**, 845 (2012).
- [31] P. J. Bustard, D. Moffatt, R. Lausten, G. Wu, I. A. Walmsley, and B. J. Sussman, *Opt. Express* **19**, 25173 (2011).
- [32] C. W. Freudiger, W. Min, B. G. Saar, S. Lu, G. R. Holtom, C. He, J. C. Tsai, J. X. Kang, and X. S. Xie, *Science* **322**, 1857 (2008).
- [33] A. Allevi, S. Olivares, and M. Bondani, *Phys. Rev. A* **85**, 063835 (2012).
- [34] A. Allevi, S. Olivares, and M. Bondani, *Int. J. Quant. Info.* **10**, 1241003 (2012).
- [35] M. Avenhaus, K. Laiho, M. V. Chekhova, and C. Silberhorn, *Phys. Rev. Lett.* **104**, 063602 (2010).
- [36] F. Haas, J. Volz, R. Gehr, J. Reichel, and J. Estève, *Science* **344**, 180 (2014).
- [37] S. K. Giri, B. Sen, C. H. Raymond Ooi, and A. Pathak, *Phys. Rev. A* **89**, 033628 (2014).

- [38] K. Thapliyal, A. Pathak, B. Sen, and J. Peřina, *Phys. Rev. A* **90**, 013808 (2014).
- [39] S. K. Giri, K. Thapliyal, B. Sen, and A. Pathak, [arXiv:1407.1780v1](https://arxiv.org/abs/1407.1780v1) [quant-ph].
- [40] K. Thapliyal, A. Pathak, B. Sen, and J. Peřina, *Phys. Lett. A* **378**, 3431 (2014).
- [41] B. Sen and S. Mandal, *J. Mod. Opt.* **52**, 1789 (2005).
- [42] B. Sen, S. Mandal, and J. Peřina, *J. Phys. B: At. Mol. Opt. Phys.* **40**, 1417 (2007).
- [43] B. Sen and S. Mandal, *J. Mod. Opt.* **55**, 1697 (2008).
- [44] B. Sen, V. Peřinová, J. Peřina, A. Lukš, and J. Křepelka, *J. Phys. B: At. Mol. Opt. Phys.* **44**, 105503 (2011).
- [45] S. Mandal and J. Perina, *Phys. Lett. A* **328**, 144 (2004).
- [46] P. Szlachetka, S. Kielich, J. Peřina, and V. Peřinová, *Opt. Acta* **27**, 1609 (1980).
- [47] D. F. Walls, *Z. Phys.* **237**, 224 (1970).
- [48] Same values of χ , g , and $|\alpha_i|$ are used in the entire paper (unless otherwise specified). For spontaneous and partially spontaneous Raman processes these values of $|\alpha_i|$ are used for nonzero $|\alpha_i|$'s.
- [49] Z.-G. Li, S.-M. Fei, Z.-X. Wang, and K. Wu, *Phys. Rev. A* **75**, 012311 (2007).
- [50] S. V. Kuznetsov, O. V. Man'ko, and N. V. Tcherniega, *J. Opt. B: Quantum Semiclass. Opt.* **5**, S503 (2003).